Int. J. Electrochem. Sci., 8 **(2013)** 7853 - 7867

International Journal of
ELECTROCHEMICAL
SCIENCE
www.electrochemsci.org

Sosedka Pegmatite Metal Ions Composition Determined by Voltammetry

Dana Fialova[1], Monika Kremplova[1], David Hynek[1,2], Marie Konecna[1,2], Jozef Kaiser[2], Radomír Malina[2], Jindrich Kynicky[3], Olga Krystofova[3], Rene Kizek[1,2], Vojtech Adam[1,2]*

[1] Department of Chemistry and Biochemistry, Faculty of Agronomy, Mendel University in Brno, Zemedelska 1, CZ-613 00 Brno, Czech Republic, European Union
[2] Central European Institute of Technology, Brno University of Technology, Technicka 3058/10, CZ-616 00 Brno, Czech Republic, European Union
[3] Karel Englis College, Sujanovo square 356/1, CZ-602 00, Brno, Czech Republic, European Union
[*]E-mail: vojtech.adam@mendelu.cz

Received: 27 March 2013 / *Accepted:* 25 April 2013 / *Published:* 1 June 2013

The aim of this study was to determine metal ions (bismuth(III), cadmium(II) and lead(II)) using differential pulse voltammetry in the sample of Sosedka pegmatite. Primarily, we characterized rock composition using electron microscopy. Further, metal ions were also determined using differential pulse voltammetry at hanging drop mercury electrode (HMDE). To determined total content of metal ions, we optimized the experimental conditions of a sample preparation as time of digestion (50 min.), amount of the sample (10 mg) and volume of digestion mixture (500 μl). In rock samples, bismuth was the most represented then it was also determined lead and a small amount of cadmium.

Keywords: Electrochemical Detection; Bismuth; Metal Ions; Geology

1. INTRODUCTION

1.1. Utilization of electrochemistry for space research

It is well known that conventional chemical and biological analyses are performed routinely on Earth, however, interplanetary investigation is still one of the major challenge. In some missions the fully automatic probes were sent and successfully landed on the surface of other planets, especially Mars [1]. In this type of a device, special technologies operating at different conditions (radiation, temperature, gravitation, atmosphere composition) are required. The Mars Environmental Compatibility Assessment (MECA) electrochemical instrument was used in Mars Lander mission [2-9]. The suggested system was based on ion sensitive electrode (ISE) sensor array. The array consisted

of 26 sensors with majority being potentiometric, but also included voltammetric, amperometric, and conductivity based devices. The potentiometric devices included ISEs based on polymer membrane and solid pellet configuration [10]. ISEs system has been studied in detail and determined to be suitable for geochemical measurements to detect different metals (Cu(II), Cd(II), Hg(II) and Pb(II)) in ppb levels using adsorptive stripping voltammetry (ASV) [11]. Moreover, Wet Chemistry Laboratory was used to determine the oxidation-reduction potential of the Phoenix WCL Rosy Red sample soil solution [12]. The electrochemically based probe was also successfully applied for *in situ* determination of heavy metals for groundwater analyses and for International Space Station water quality measurements [13]. The analytical performance of the in situ probe consisting of a microlithographically fabricated iridium or gold ultramicroelectrode array sensors was studied by using square wave anodic stripping voltammetry [14-17]. Herdan's study demonstrates that such electroanalytical-based devices may be of value for an initial, rapid, low-cost, screening of heavy metal contaminated sites [14].

Unique LCT (lithium – caesium – tantalum) granites and pegmatites of Malkhan Ridge were discovered in Chita Oblast of Central Transbaikalia. The Malkhan pegmatite field occupies an area of 60 km^2. In the early 1980s, a large deposit of gem quality liddicoatite and elbaite (pink rubellite and green verdelite varieties) was found in this field. In addition, the associated crystal bearing miaroles contain also gem-quality beryl (morganite), garnet, danburite, hambergite, pollucite, and smoky quartz [18]. This large pegmatite field is located 250 km to the South-East of Ulan-Ude, capital of Buryat Republic, just above the border with Mongolia. The geology of the Malkhan field, composition, and internal structure of pegmatites were previously characterized in [19,20]. The Malkhan pegmatite field comprises more than 350 pegmatite dykes and veins. Almost 50 pegmatites contained pockets with gem mineralization. There were found definitely the best gemmy pink and violet elbaite and liddicoatite specimens worldwide. But those pegmatites and namely Sosedka pegmatite vein are also the source of the largest known native bismuth crystals and clusters of aggregates and breccias rich in several rare Nb – Ta – Sn – rare-earth elements (REE) bearing minerals like bismutocolumbite, cassiterite, columbite-(Mn), euxenite-(Y), ixiolite, scandian ixiolite, bismutomicrolite, monazite-(Ce), polycrase-(Y), pyrochlore, betafite, stibiomicrolite and xenotime-(Y). A detailed study was given to the composition and structure of alkali feldspars from the pockets of the Sosedka pegmatite vein, a large source of gems within the Malkhan tourmaline deposit. The vein is of concentric-zonal structure. Three types of pockets were recognized by mineral composition: A-quartz-lepidolite-Mn-Li-Al-tourmaline (+/- pollucite, hambergite, borocookeite, boromuscovite, danburite, light pink beryl); B-quartz-adularia-axinite (+/- laumontite); and C-quartz and laumontite (+/- B-containing cookeite). Each type of pockets contains feldspars of specific composition and structure [21].

1.2. Sosedka pegmatite body as a source of critical and rare metal mineralization

The most important and productive pegmatite body is named Sosedka, which is the source of lithium, scandium, tantalum and bismuth mineralization. Sosedka pegmatite is located at 50°39′06′′N,

109°53′14′′E. The own pegmatite represents a slightly dipping lenticular body more than 400 m long and up to 45 m thick hosted by metadiorites. The pegmatite consists of graphic, sub-graphic, and irregularly distributed pegmatoidal quartz–oligoclase and quartz–potassium feldspar with accessory distributed schorl, biotite and almandine–spessartine garnet. Subordinate are parts of blocky and near-pocket feldspar and quartz, as well as quartz–tourmaline–lepidolite–albite-bimust-bismutite assemblages. The volume of the pockets varies from cubic centimetres to 16 cubic meters. Bismut-tantalum mineralization is present in all pegmatite zones, even in the vicinity of the contacts with host rocks, without any regularity. The largest clusters of bismuth mineralization associated with miarolitic cavities were found in 2010 and 2012. While the first miarol and near miarolitic mineral associations were full of bismuth in breccia cemented by bismuth-albite mineralization, the latest almost independent miarol in the bottom of „bubbles like miarolitic cluster was found in late September 2012. It was almost 3 m long (2 m^3), lined up with fresh crystals, mainly quartz crystals (smoky quartz) up to 0,5m in length. Crystals of white K-feldspar were slightly corroded by younger hydrothermal fluids. Albite appears in variety cleavelandite and was associated with purple tabular crystals of lepidolite. Crystals of tourmaline were composed of schorl base followed by yellow zone, pink to multicolored core and liddicoatite rim. Stilbite, laumontite and axinite crystals were found as modally important accesory minerals. Those minerals belong to the late stage magmatic mineralization of miaroles. Late hydrothermal mineralization stage was represented mainly by zeolites (stilbite, laumontite) in lesser extent by axinite and adularia.

The aim of this study was to focus on the application of portable electrochemical detection for the analysis of the mineral sample with one prevailing major element and the evaluation of technical possibilities of sample preparation for automated analysis with potential application in planetary exploration program.

2. EXPERIMENTAL PART

2.1. X-ray computed tomography

We used microtomographic station GE v|tome|x L240 with a 180 kV nanofocus tube (GE Phoenix X-ray, Germany). The tube voltage was set to 160 kV and tube current to 40 μA. The resolution of the tomographic reconstruction reached up to 6.5 μm.

2.2. Electron microscope analysis

The FEG-SEM TESCAN MIRA 3 XMU (Czech Republic) was used for high quality documentation of the bismuth samples on doubly polished thin sections. This MIRA 3 XMU model was equipped with a high brightness Schottky field emitter for low noise imaging at fast scanning

rates. The SEM was fitted with Everhart-Thronley type of SE detector, high speed YAG scintillator based BSE detector, panchromatic CL Detector and EDX spectrometer Bruker Quantax 800 (Germany) or Oxford Instruments XMax 80 (UK). The MIRA 3 XMU system is based on a large specimen chamber with motorized stage movements 130x130 mm i.e. up to 10 slides can be load in for one analysis. Samples were coated by 15 nm of carbon to prevent sample charging. A carbon coater Quorum Technologies K950X was used. For automated acquisition of large areas a TESCAN proprietary software tool called Image Snapper was used. The software enables automatic acquisition of selected areas with defined resolution. Different conditions were tested for acquisition in order to reach either minimum analysis time or maximum detail during overnight automated analyses. Typically an accelerating voltage of 25 kV and beam currents about 5 nA gives satisfactory results.

2.3. Chemicals and material

All chemicals used were purchased from Sigma Aldrich (St. Louis, MA, USA) in ACS purity unless noted otherwise. Stock solutions were prepared with ACS water. pH value and conductivity was measured using inoLab Level 3 (Wissenschaftlich-Technische Werkstatten; Weilheim, Germany). Deionized water underwent demineralization by reverse osmosis using Aqua Osmotic 02 (Aqua Osmotic, Tisnov, Czech Republic) and was subsequently purified using Millipore RG (MilliQ water, 18 MΩ, Millipore, Billerica, MA, USA). Deionized water was used for rinsing, washing, and buffer preparation.

2.4. Sample preparation

Primarily, the pegmatite fragments were crushed to small pieces and then reduced to a powder consistency. 10 and 100 mg of this powder was weighted into digestion vials. Nitric acid (65 %) and hydrogen peroxide (30 %) were used as the digestion mixture. There were used two different volumes of digestion mixture – 500 and 1000 µl, while the ratio between nitric acid and hydrogen peroxide was always 7:3. Samples were digested by using Microwave 3000 (Anton-PaarGmbH, Austria) and two different time periods were applied: 50 minutes digestion (50 W-10 minutes, 100 W-30 minutes, 0 W (cooling)-10 minutes, IR 140°C) and 70 minutes digestion (50 W-10 minutes, 100 W-50 minutes, 0 W (cooling)-10 minutes, IR 140°C). After the digestion, the samples with digestion mixture were pipetted into Eppendorf vials and electrochemical determination of bismuth, lead and cadmium followed [22-26].

2.5. Electrochemical detection of bismuth, lead and cadmium

Electrochemical measurements were performed using 797 VA Computrace connected to 889 IC Sample Center (Metrohm, Switzerland) using a standard cell with three electrodes. A hanging

mercury drop electrode (HMDE) with a drop area of 0.4 mm^2 was the working electrode. An Ag/AgCl/3M KCl electrode was the reference and platinum electrode was the auxiliary. The analyzed samples were deoxygenated prior to measurements by purging with argon (99.999 %). Acetate buffer (0.2 M CH_3COONa and CH_3COOH, pH 5) was used as a supporting electrolyte. The supporting electrolyte was exchanged after each analysis. The parameters of the measurement were as follows: initial potential of -1.1 V, end potential 0.2 V, purging with argon 120 s, deposition potential -1.1 V, accumulation time 800 s, equilibration time 5 s, pulse amplitude 0.025 V, pulse time 0.05 s, voltage step 2 mV, voltage step time 0.2 s, sweep rate 0.01 V/s, sample volume: 20 µl, volume of measurement cell: 2 ml (20 µl of sample and 1980 µl acetate buffer).

2.6. Descriptive statistics

Data were processed using MICROSOFT EXCEL (Microsoft, Redmond, WA, USA) and STATISTICA.CZ Version 8.0 (Stat-Soft CR, Prague, Czech Republic). The results are expressed as mean ±SD unless otherwise noted. The detection limits (3 S/N) were calculated according to Long and Winefordner [27], whereas N was expressed as a standard deviation of noise determined in the signal domain unless otherwise stated.

3. RESULTS AND DISCUSSION

3.1. Tomography and microscope results

With the development of variety of spectroscopic techniques the preparation of the sample is, at least partially, eliminated. These techniques usually involve the source of energy which bombards the surface of the sample. This process produces the signal that can be measured. For this purpose, before analysis the sample is cut and polished, or powdered and pressed into the form of the tablet. The most applied methods are X-ray fluorescence (XRF) or X-ray diffractometry (XRD) and also scanning electron microscopy (SEM) and electron probe microanalysis (EPMA), the non-destructive methods for the analysis of the surface and subsurface layers of minute solid samples [28,29]. Non-destructive means the analysis does not lead to volume loss of the sample, so it is possible to re-analyse the same materials more than one time. The significant group of analytical methods in elemental mapping is based on laser-assisted sampling. The result of Laser-Induced Breakdown Spectroscopy (LIBS) or Laser Ablation Inductively Coupled Plasma Optical Emission Spectrometry or Mass Spectrometry (LA-ICP-OES/MS) is the information about the element line intensity (or area) versus one or more spatial coordinates. The images of the spatial distribution serve to establish compositional interrelationships of the elemental constituents in the sample [30-38]. In this type of geological samples beside major and minor elements, trace levels of contaminants are very often determined due to pollution, which may be an indicator in ecological investigation [39]. These elements require highly

sensitive and element specific analytical methods. The limits of detection of above mentioned methods are unfortunately higher in comparison with traditional analytical techniques or the quantification is not possible due to the absence of calibration standards and too many matrix interferences.

For our experiment, X-ray computed tomography (CT) was chosen as a powerful non-destructive imaging technique, where individual projections (radiographs) recorded from different viewing directions are used to reconstruct the three-dimensional insight (cross-section) of the inner structure of the object of interest [40,41]. High-resolution X-ray CT is also termed microComputed Tomography (microCT, μCT) or microtomography and reconstructs samples interiors with the spatial and contrast resolution with a voxel size in the micrometre range that is required for many problems of interest. By suitable processing, it is possible to detect the presence of defects, to identify internal structures and to study their form and position, to quantify density variations, and to model the components of the object. Due to high absorption of the sample, only small part (3.2 × 5.7 × 6.4 mm and total volume 42.7 mm^3) was scanned. Fig. 1A shows a rendered 3D view of the partial section of the sample. Cross-section of the sample in the y-z plane is shown in Fig. 1B. It is obvious that inside the volume there is no significant inner structure visible, except some small veins in the bottom-left corner of Fig. 1B.

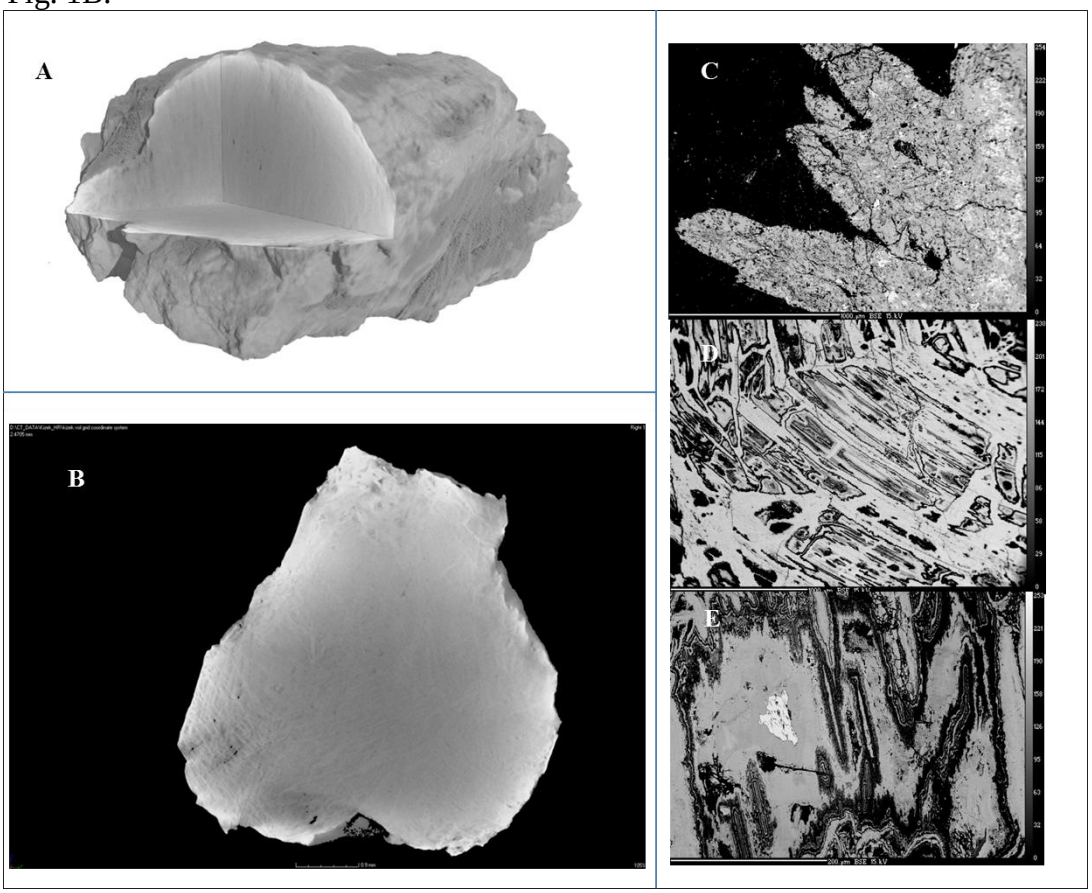

Figure 1. (**A**) Rendered 3D view of the partial section of the sample. (**B**) Cross-section of the sample in the y-z plane. It is obvious that inside the volume there is no significant inner structure visible, except some small veins in the bottom-left corner. (**C**-**E**) SEM pictures.

Area of the thin section (26×48 mm) can be divided to 9×17 tiles with 3 mm field of view. An overlap 10% between tiles was used. This makes 153 tiles in total. Using the image resolution e.g. 2048×2048 pixels we can reach a the image with detail about 1.5 μm. Acquisition time when using pixel dwell time 1 μs would be around 25 minutes. (For image resolution 1024×1024 the image detail would be 3 μm and acquisition time 7 minutes). This method of operation was used for high quality and detail documentation of the bismuth samples on doubly polished thin sections (Fig. 1C). Native bismuth on the panoramatic image is partially altered to younger/secondary oxide and carbonate Bi minerals (Bismutine, bismutit, and others). The newly formed layered and mosaic texture is well documented. The porous micro texture is the reason for caption of other heavy metals. Bismuth forms both large yellowish crystals and huge crystal aggregates up to 30 cm in diameter (Fig. 1D). Individual fresh crystals display an intense metallic lustre, while breccia aggregates are usually intensively corroded and altered. Aggregates of native bismuth are associated with albite and the latest generation of tourmaline. Those aggregates are mostly altered and newly formed bismite replace it from rims to core. Bismuth powder diffraction data closely match the theoretical data calculated from the structure of bismuth and data reported in the literature for this mineral specie. Bismite is volumetrically the most abundant part of the studied bismuth mineralization. It is mostly grey, sometimes slightly greenish in colour. It encloses relict aggregates of pure bismuth, albite and Bi enriched Li-tourmaline. Powder diffraction record bismite very well with theoretical data calculated from the crystal structure. Minor differences in the intensity of the record are probably caused by texture analysis preparation. Chemical composition of bismite from Sosedka pegmatite corresponds to the empirical formula. Bismutite forms massive aggregates in bismite. Both bismutite and bismite are alteration products after native bismuth. Bismutite is always intimately interconnects with bismite (many coincidences) so the clear lattice parameters of the mineral phase are rare (Fig. 1E).

3.2. Electrochemical detection of heavy metals at HMDE

Heavy metals ions are nowadays commonly detected in solid and liquid samples using electrochemical methods. Heavy metals can be determined on glassy carbon (GC), hanging mercury drop electrode (HMDE) or carbon paste electrode (CPE) [23,24,42-45]. Determination of metals in samples of stone from the area of Siberia was done using 797 VA Computrace (Metrohm, Switzerland) with automatic sample dispensing apparatus secured 889 IC Sample Center (Metrohm, Switzerland). Primarily, we determined the calibration curve for each metal of interest. For detection of bismuth(III), lead(II) and cadmium(II) ions differential pulse voltammetry was applied.

The obtained concentration dependence for bismuth(III) was linear within the range from 0.009 μg/ml to 100 μg/ml as it follows: $y = 9.520x$; $R^2 = 0.999$, n = 3, R.S.D = 1.24 % (Fig. 2A and Table 1). The obtained concentration dependence for lead(II) was linear within the range from 0.012 μg/ml to 100 μg/ml as it follows: $y = 7.783x$; $R^2 = 0.999$, n = 3, R.S.D = 3.14 % (see Fig. 2B and Table 2). The obtained concentration dependence for cadmium(II) was linear within the range from 0.67 ng/ml to

2810 ng/ml as it follows: y = 0.725x; R^2 = 0.992, n = 3, R.S.D = 0.82 % (see Fig. 2C and Table 3). The changes in peak potentials were negligible (upper insets in Figs. 2A, B and C).

Table 1. Analytical parameters of electrochemical determination of Bi(III).

Substance	Regresion equation	Linear dynamic range	Linear dynamic range	R2[1]	LOD[2]	LOD	LOQ[3]	LOQ	RSD[4]
		(μM)	(μg/ml)		(μM)	(μg/ml)	(μM)	(μg/ml)	(%)
Bi	y = 9.520x	0.43 – 478	0.09 – 100	0.999	0.1	0.03	0.5	0.1	1.24

1…regression coefficients
2…limits of detection of detector (3 S/N)
3… limits of quantification of detector (10 S/N)
4…relative standard deviations

Table 2. Analytical parameters of electrochemical determination of Pb(II).

Substance	Regresion equation	Linear dynamic range	Linear dynamic range	R2[1]	LOD[2]	LOD	LOQ[3]	LOQ	RSD[4]
		(μM)	(μg/ml)		(μM)	(μg/ml)	(μM)	(μg/ml)	(%)
Pb	y = 7. 7825x	0.058 – 482	0.012 – 100	0.999	0.01	0.002	0.03	0.007	3.14

1…regression coefficients
2…limits of detection of detector (3 S/N)
3… limits of quantification of detector (10 S/N)
4…relative standard deviations

Table 3. Analytical parameters of electrochemical determination of Cd(II).

Substance	Regresion equation	Linear dynamic range	Linear dynamic range	R2[1]	LOD[2]	LOD	LOQ[3]	LOQ	RSD[4]
		(μM)	(ng/ml)		(nM)	(ng/ml)	(nM)	(ng/ml)	(%)
Cd	y = 81.48x	0.006 – 25	0.67 – 2810	0.992	0.2	0.018	0.5	0.06	0.82

1…regression coefficients
2…limits of detection of detector (3 S/N)
3… limits of quantification of detector (10 S/N)
4…relative standard deviations

3.3. The effect of sample preparation on the electrochemical determination

Chemical analysis of rock and mineral samples is usually based on the application of different detection techniques used after preliminary preparation step or in-situ. The most common procedure of sample preparation is dissolving of the mineral in various acids or their mixtures [46]. Usually the determination of elements is realized by wet chemistry step coupled with a suitable detection technique. Wet chemistry includes decomposition of the sample with typical inorganic acids (HNO_3, HCl, HF, H_2SO_4, $HClO_4$). Conventional heating of samples was replaced by the use microwaves [25,47,48]. Microwave heating ensures elimination of contamination, and it improves the speed and efficiency of digestion for some types of samples considered difficult to solubilize. Microwave heating also prevents the losses of the volatile species or elements, such as As or Se [49]. This kind of

digestion is advantageous for silicate matrix decomposition. The process is not only dependent on the used mineral acid and its volume, but also on the time and power of microwaves therefore the optimization is necessary [50,51]. The analyses of metals in the decomposed samples are based on spectroscopic techniques, such as atomic absorption spectrometry (AAS) [52,53] and inductively coupled plasma optical emission or mass spectrometry (ICP-OES; ICP-MS respectively) [54,55]. Beside the optical techniques are electrochemical methods successfully applied for simultaneous determination of several metal ions in biological or environmental samples [23,24]. Among the different electrochemical techniques voltammetric and potentiometric techniques are the most reported for heavy metals detection [56-60]. In addition to conventional hanging mercury drop electrode the most commonly used electrode material for the detection of metals is carbon. Determination of metals on the electrodes made of different modifications of carbon (tips, rods, glassy carbon, carbon paste with different content of carbon particles with various shapes and sizes) can be found elsewhere [61-63]. Electrochemical deposition of the analyte on electrodes can be utilized as a special technique for the separation of the analyte from the matrix. During the electrochemical deposition the analyte ions are separated from the sample matrix and can also be preconcentrated. Analyte deposited on the electrode can be treated in several manners. Trace metals (Cd, Cu, Pb, Ni, Cr, Au) electrochemically deposited on the graphite atomizer surface were determined by electrothermal AAS [64-66].

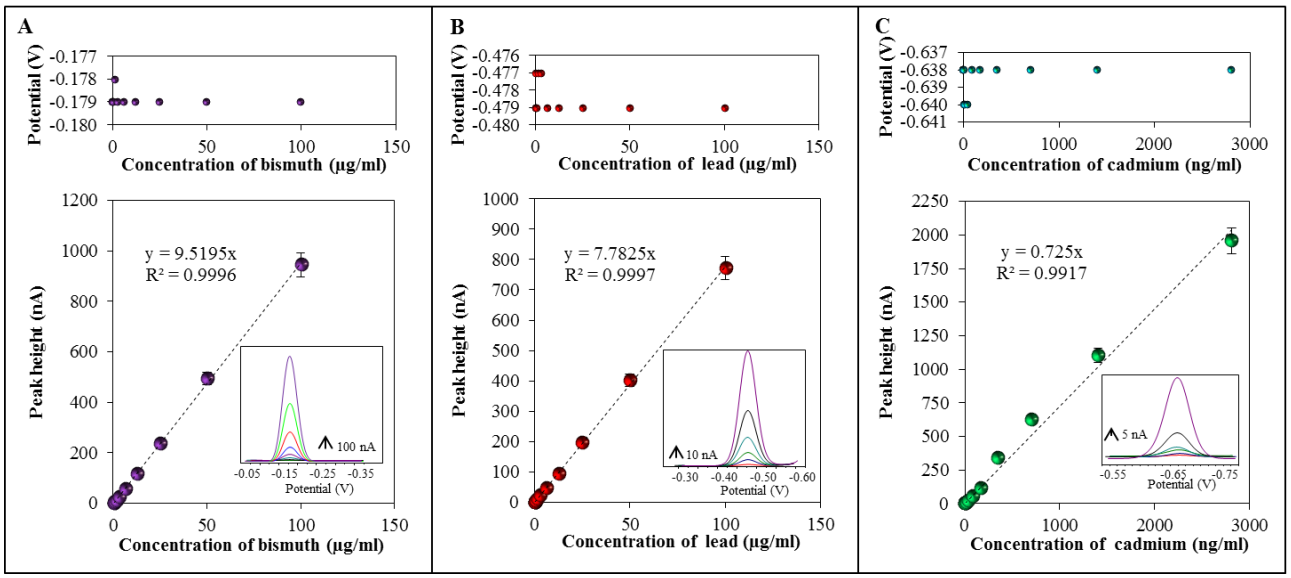

Figure 2. Calibration curves of (**A**) bismuth(III), (**B**) lead(II) and (**C**) cadmium(II) determined by DPV. There is dependence of potential on metal concentration above each calibration curve. 0.2 M acetate buffer (pH=5) was used as an electrolyte. The experimental parameters were as it follows: initial potential -1.1 V, end potential 0.2 V, deposition potential -1.1 V, accumulation time 720 s, pulse amplitude 25 mV, pulse time 0.05 s, voltage step 1.984 mV, voltage step time 0.2 s, sweep rate 0.0099 V/s.

Electrochemical determination of metal ions from rock samples requires decomposition of solid matrix to the liquid state. This procedure can be made by various ways. In our case microwave

digestion was applied for preparation of small amount of sample according to protocol mentioned in the cited papers [22,23]. Parameters of this procedure were optimized for obtaining the best results for metals electrochemical detection. They were primarily the portion of the sample, the ratio and the amount of digestion mixture and also the time and digestion power.

The samples were divided into several groups according to sample weight (10 or 100 mg), the volume of digestion mixture (500 and 1000 µl) and the time of digestion program (50 and 70 minutes). The volume of digestion mixture influenced the resulting metal concentration in the samples. Therefore the evaluation of this parameter impact to the electrochemical detection of individual ions was corrected with dilution factor. In generally, the increasing volume of digestion mixture led to the increase of electrochemical signal, in both applied dosage (10 and 100 mg) of samples (Figs. 3A and B, respectively). All values were related to the maximum value. The greatest difference is visible at bismuth detection in the case of 100 mg dosage. The difference between 500 and 1000 µl of applied digestion mixture created about 50% of detected electrochemical signal (Fig. 3B). Determination of lead using 100 mg of sample and 1000 µl of digestion mixture led to the increasing of electrochemical signal according to applying 500 µl of digestion mixture up to 8%. Other experimental conditions led to the negligible changes in obtained electrochemical signals. In addition, for all metals, the current response decreased with the longer digestion time. On the other hand, with application 100 mg of sample (Fig. 3B) this trend changed to the other side, and electrochemical signals grew with longer digestion time the. This phenomenon is probably caused by the large amount of sample in the digestion mixture. 50 min of digestion program seems not to be enough.

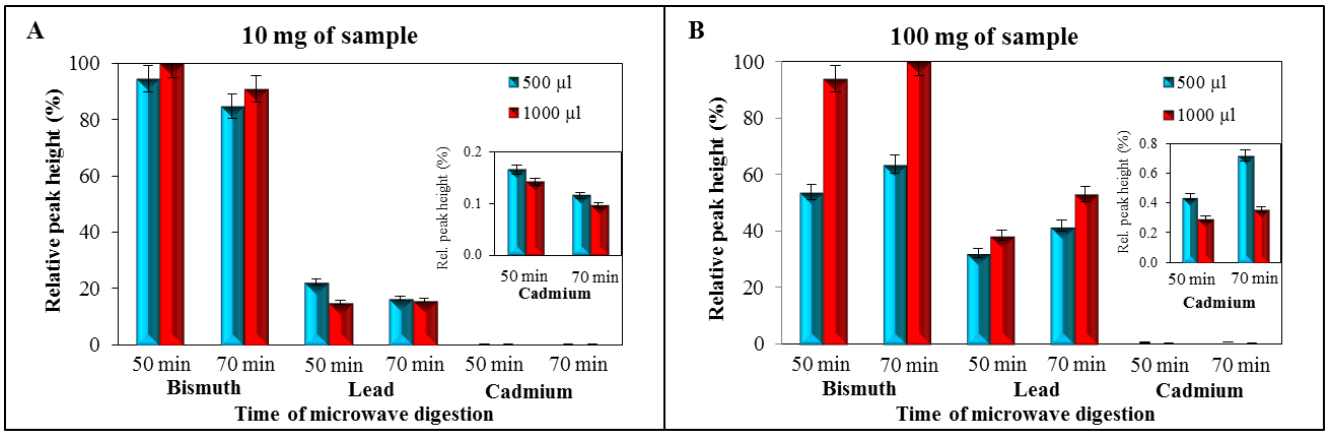

Figure 3. Microwave digestion process, the dependence of digestion time on relative peak height detected by DPV for individual metal ions contained in the sample. (**A**) Relative peak height of bismuth, lead and cadmium in 10 mg of sample, digestion times 50 and 70 minutes, volume of digestion mixture was 500 or 1000 µl. (**B**) Relative peak height of bismuth, lead and cadmium in 100 mg of sample, digestion times were 50 and 70 minutes, volume of digestion mixture was 500 or 1000 µl.

Application of 10 mg of samples to digestion process led to the formation well developed and symmetric peaks for bismuth and lead. The bismuth peak was located at potential about - 0.18 V. The peak position showed no change according to the calibration curve position peaks. Lead peaks were located at -0.48 V and cadmium peaks at -0.65 V. The growing amount of using sample (100 mg) for the digestion process led to the change of bismuth detected peak. The electrochemical signal of lead had no changes due to using 100 mg of dosage sample. Cadmium peaks showed no changes with changing sample amount and theirs position had no changes too. Based on the previously mentioned results, the following optimal conditions were selected: the portion of 100 mg, 70 minutes of digestion process and the volume of the digestion mixture 1000 µl showed as the best conditions for 100 mg of sample digestion.

3.4. Electrochemical detection of heavy metals in Sosedka pegmatite

Our experiment was based on electrochemical determination of heavy metal ions in Sosedka pegmatite using differential pulse voltammetry. This determination was done on mercury electrode for which the microwave digestion of solid sample in acids mixture was chosen. The total content of metals determined in a sample of stone from the area of Siberia is shown in Fig. 4. Bismuth was determined nearly as 11 mg/g. The lead content was determined to be 3 mg/g, and the last detected metal was cadmium as 0.3 µg/g. It is obvious that analysed sample composed in majority from bismuth and lead. Minor of the composition is created with cadmium, which is in thousands lower than bismuth and lead concentration. It was showed that the application of electrochemical methods in combination with microwave digestion of solid samples is possible and useful tool for heavy metal determination.

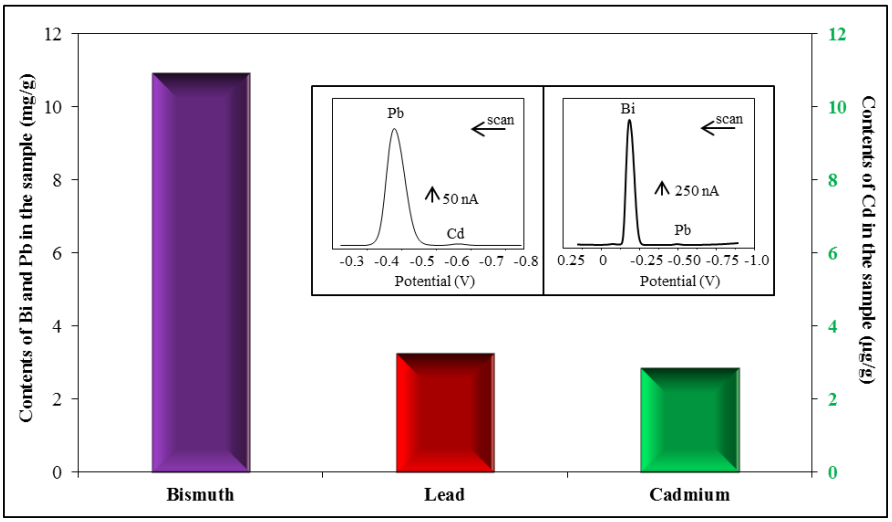

Figure 4. Contents of bismuth (mg/g), lead (mg/g) and cadmium (µg/g) in the real sample of the Siberian mineral determined with DPV method (obtained voltammograms are presented as inset pictures).

4. CONCLUSION

Interplanetary exploration will require new technologies that facilitate detection of selected metal ions, microbial activity and biomolecules. Development of well portable, robust, sensitive and low cost of can be beneficial for geological and planetary exploration program [2]. Therefore, one may expect that further development of electrochemical detectors usable in mobile robotic devices will be required [2,67-72].

ACKNOWLEDGEMENTS
Financial support from IGA VSKE 2013 and CEITEC CZ.1.05/1.1.00/02.0068 is highly acknowledged.

References

1. S. P. Kounaves and M. H. Hecht, *Geochim. Cosmochim. Acta*, 66 (2002) A413.
2. S. P. Kounaves, *ChemPhysChem*, 4 (2003) 162.
3. S. J. West, M. S. Frant, X. W. Wen, R. Geis, J. Herdan, T. Gillette, M. H. Hecht, W. Schubert, S. Grannan and S. P. Kounaves, *Am. Lab.*, 31 (1999) 48.
4. S. P. Kounaves, S. R. Lukow, B. P. Comeau, M. H. Hecht, S. M. Grannan-Feldman, K. Manatt, S. J. West, X. W. Wen, M. Frant and T. Gillette, *J. Geophys. Res.-Planets*, 108 (2003) 1.
5. W. V. Boynton, D. W. Ming, S. P. Kounaves, S. M. M. Young, R. E. Arvidson, M. H. Hecht, J. Hoffman, P. B. Niles, D. K. Hamara, R. C. Quinn, P. H. Smith, B. Sutter, D. C. Catling and R. V. Morris, *Science*, 325 (2009) 61.
6. M. H. Hecht, S. P. Kounaves, R. C. Quinn, S. J. West, S. M. M. Young, D. W. Ming, D. C. Catling, B. C. Clark, W. V. Boynton, J. Hoffman, L. P. DeFlores, K. Gospodinova, J. Kapit and P. H. Smith, *Science*, 325 (2009) 64.
7. S. P. Kounaves, M. H. Hecht, J. Kapit, K. Gospodinova, L. DeFlores, R. C. Quinn, W. V. Boynton, B. C. Clark, D. C. Catling, P. Hredzak, D. W. Ming, Q. Moore, J. Shusterman, S. Stroble, S. J. West and S. M. M. Young, *J. Geophys. Res.-Planets*, 115 (2010) 1.
8. S. P. Kounaves, M. H. Hecht, S. J. West, J. M. Morookian, S. M. M. Young, R. Quinn, P. Grunthaner, X. W. Wen, M. Weilert, C. A. Cable, A. Fisher, K. Gospodinova, J. Kapit, S. Stroble, P. C. Hsu, B. C. Clark, D. W. Ming and P. H. Smith, *J. Geophys. Res.-Planets*, 114 (2009) 1.
9. P. H. Smith, L. K. Tamppari, R. E. Arvidson, D. Bass, D. Blaney, W. V. Boynton, A. Carswell, D. C. Catling, B. C. Clark, T. Duck, E. DeJong, D. Fisher, W. Goetz, H. P. Gunnlaugsson, M. H. Hecht, V. Hipkin, J. Hoffman, S. F. Hviid, H. U. Keller, S. P. Kounaves, C. F. Lange, M. T. Lemmon, M. B. Madsen, W. J. Markiewicz, J. Marshall, C. P. McKay, M. T. Mellon, D. W. Ming, R. V. Morris, W. T. Pike, N. Renno, U. Staufer, C. Stoker, P. Taylor, J. A. Whiteway and A. P. Zent, *Science*, 325 (2009) 58.
10. K. McElhoney, G. D. O'Neil, N. A. Chaniotakis and S. P. Kounaves, *Electroanalysis*, 24 (2012) 2071.
11. M. A. Nolan and S. P. Kounaves, *Anal. Chem.*, 71 (1999) 3567.
12. R. C. Quinn, J. D. Chittenden, S. P. Kounaves and M. H. Hecht, *Geophys. Res. Lett.*, 38 (2011) 1.
13. M. G. Buehler, G. M. Kuhlman, D. Keymeulen, N. V. Myung and S. P. Kounaves, in 2003 IEEE Aerospace Conference Proceedings, Vols 1-8, IEEE, New York, 2003, p. 535.

14. J. Herdan, R. Feeney, S. P. Kounaves, A. F. Flannery, C. W. Storment, G. T. A. Kovacs and R. B. Darling, *Environ. Sci. Technol.*, 32 (1998) 131.
15. R. Feeney, J. Herdan, M. A. Nolan, S. H. Tan, V. V. Tarasov and S. P. Kounaves, *Electroanalysis*, 10 (1998) 89.
16. R. Feeney and S. P. Kounaves, *Electroanalysis*, 12 (2000) 677.
17. R. Feeney and S. P. Kounaves, *Anal. Chem.*, 72 (2000) 2222.
18. E. Badanina, V. Gordienko, A. Wiechowski and G. Friedrich, *Geol. Ore Depos.*, 50 (2008) 772.
19. I. S. Peretyazhko, V. Y. Zagorsky, S. Z. Smirnov and M. Y. Mikhailov, *Chem. Geol.*, 210 (2004) 91.
20. R. Thomas, P. Davidson and E. Badanina, *Minerals*, 2 (2012) 435.
21. V. Y. Zagorsky, *Russ. Geol. Geophys.*, 53 (2012) 522.
22. D. Hynek, L. Krejcova, S. Krizkova, B. Ruttkay-Nedecky, J. Pikula, V. Adam, P. Hajkova, L. Trnkova, J. Sochor, M. Pohanka, J. Hubalek, M. Beklova, R. Vrba and R. Kizek, *Int. J. Electrochem. Sci.*, 7 (2012) 943.
23. D. Hynek, J. Prasek, J. Pikula, V. Adam, P. Hajkova, L. Krejcova, L. Trnkova, J. Sochor, M. Pohanka, J. Hubalek, M. Beklova, R. Vrba and R. Kizek, *Int. J. Electrochem. Sci.*, 6 (2011) 5980.
24. A. Kleckerova, P. Sobrova, O. Krystofova, J. Sochor, O. Zitka, P. Babula, V. Adam, H. Docekalova and R. Kizek, *Int. J. Electrochem. Sci.*, 6 (2011) 6011.
25. M. Kremplova, L. Krejcova, D. Hynek, P. Barath, P. Majzlik, V. Horak, V. Adam, J. Sochor, N. Cernei, J. Hubalek, R. Vrba and R. Kizek, *Int. J. Electrochem. Sci.*, 7 (2012) 5893.
26. P. Majzlik, A. Strasky, V. Adam, M. Nemec, L. Trnkova, J. Zehnalek, J. Hubalek, I. Provaznik and R. Kizek, *Int. J. Electrochem. Sci.*, 6 (2011) 2171.
27. G. L. Long and J. D. Winefordner, *Anal. Chem.*, 55 (1983) A712.
28. L. Q. Luo, B. B. Chu, Y. C. Li, T. Xu, X. F. Wang, J. Yuan, J. L. Sun, Y. Liu, Y. Bo, X. C. Zhan, S. X. Wang and L. J. Tang, *X-Ray Spectrometry*, 41 (2012) 133.
29. M. Miro, E. H. Hansen, R. Chomchoei and W. Frenzel, *Trac-Trends in Analytical Chemistry*, 24 (2005) 759.
30. J. Kaiser, K. Novotny, M. Z. Martin, A. Hrdlicka, R. Malina, M. Hartl, V. Adam and R. Kizek, *Surf. Sci. Rep.*, 67 (2012) 233.
31. G. Vitkova, K. Novotny, L. Prokes, A. Hrdlicka, J. Kaiser, J. Novotny, R. Malina and D. Prochazka, *Spectroc. Acta Pt. B-Atom. Spectr.*, 73 (2012) 1.
32. M. Galiova, J. Kaiser, F. J. Fortes, K. Novotny, R. Malina, L. Prokes, A. Hrdlicka, T. Vaculovic, M. N. Fisakova, J. Svoboda, V. Kanicky and J. J. Laserna, *Appl. Optics*, 49 (2010) C191.
33. E. A. Belousova, W. L. Griffin, S. Y. O'Reilly and N. I. Fisher, *J. Geochem. Explor.*, 76 (2002) 45.
34. J. Kaiser, M. Galiova, K. Novotny, R. Cervenka, L. Reale, J. Novotny, M. Liska, O. Samek, V. Kanicky, A. Hrdlicka, K. Stejskal, V. Adam and R. Kizek, *Spectrochim. Acta, Part B*, 64 (2009) 67.
35. O. Krystofova, V. Shestivska, M. Galiova, K. Novotny, J. Kaiser, J. Zehnalek, P. Babula, R. Opatrilova, V. Adam and R. Kizek, *Sensors*, 9 (2009) 5040.
36. M. Galiova, J. Kaiser, K. Novotny, M. Hartl, R. Kizek and P. Babula, *Microsc. Res. Tech.*, 74 (2011) 845.
37. M. Ryvolova, J. Chomoucka, J. Drbohlavova, P. Kopel, P. Babula, D. Hynek, V. Adam, T. Eckschlager, J. Hubalek, M. Stiborova, J. Kaiser and R. Kizek, *Sensors*, 12 (2012) 14792.
38. L. Krajcarova, K. Novotny, P. Babula, I. Provaznik, P. Kucerova, V. Adam, M. Z. Martin, R. Kizek and J. Kaiser, *Int. J. Electrochem. Sci.*, in press (2013).
39. P. Byrne, P. J. Wood and I. Reid, *Crit. Rev. Environ. Sci. Technol.*, 42 (2012) 2017.

40. J. Kaiser, L. Reale, A. Ritucci, G. Tomassetti, A. Poma, L. Spano, A. Tucci, F. Flora, A. Lai, A. Faenov, T. Pikuz, L. Mancini, G. Tromba and F. Zanini, *Eur. Phys. J. D*, 32 (2005) 113.
41. J. Kaiser, M. Hola, M. Galiova, K. Novotny, V. Kanicky, P. Martinec, J. Scucka, F. Brun, N. Sodini, G. Tromba, L. Mancini and T. Koristkova, *Urol. Res.*, 39 (2011) 259.
42. V. Adam, O. Zitka, D. Huska, S. Krizkova, J. Strnadel, V. Horak, T. Vaculovic, K. Novotny, V. Kanicky, J. Kaiser and R. Kizek, *FEBS J.*, 276 (2009) 96.
43. D. Huska, O. Zitka, V. Adam, M. Beklova, S. Krizkova, L. Zeman, A. Horna, L. Havel, J. Zehnalek and R. Kizek, *Czech J. Anim. Sci.*, 52 (2007) 37.
44. P. Majzlik, J. Prasek, L. Trnkova, J. Zehnalek, V. Adam, L. Havel, J. Hubalek and R. Kizek, *Lis. Cukrov. Repar.*, 126 (2010) 413.
45. J. Sochor, P. Majzlik, P. Salas, V. Adam, L. Trnkova, J. Hubalek and R. Kizek, *Lis. Cukrov. Repar.*, 126 (2010) 414.
46. D. Carroll and H. C. Starkey, *Clay Clay Min.*, 19 (1971) 321.
47. O. Krystofova, O. Zitka, S. Krizkova, D. Hynek, V. Shestivska, V. Adam, J. Hubalek, M. Mackova, T. Macek, J. Zehnalek, P. Babula, L. Havel and R. Kizek, *Int. J. Electrochem. Sci.*, 7 (2012) 886.
48. O. Krystofova, V. Adam, P. Babula, J. Zehnalek, M. Beklova, L. Havel and R. Kizek, *Int. J. Environ. Res. Public Health*, 7 (2010) 3804.
49. S. Garcia-Salgado, M. A. Quijano and M. M. Bonilla, *Anal. Chim. Acta*, 714 (2012) 38.
50. V. Sandroni and C. M. M. Smith, *Anal. Chim. Acta*, 468 (2002) 335.
51. C. Bettiol, L. Stievano, M. Bertelle, F. Delfino and E. Argese, *Appl. Geochem.*, 23 (2008) 1140.
52. V. N. Oreshkin and G. I. Tsizin, *J. Anal. Chem.*, 67 (2012) 830.
53. P. Pohl, *Trac-Trends in Analytical Chemistry*, 28 (2009) 117.
54. N. N. Fedyunina, K. B. Ossipov, I. F. Seregina, M. A. Bolshov, M. A. Statkus and G. I. Tsysin, *Talanta*, 102 (2012) 128.
55. N. N. Fedyunina, I. F. Seregina, M. A. Bolshov, O. I. Okina and S. M. Lyapunov, *Anal. Chim. Acta*, 713 (2012) 97.
56. G. Aragay and A. Merkoci, *Electrochim. Acta*, 84 (2012) 49.
57. J. F. Ping, J. Wu, Y. B. Ying, M. H. Wang, G. Liu and M. Zhang, *J. Agric. Food Chem.*, 59 (2011) 4418.
58. S. Krizkova, P. Ryant, O. Krystofova, V. Adam, M. Galiova, M. Beklova, P. Babula, J. Kaiser, K. Novotny, J. Novotny, M. Liska, R. Malina, J. Zehnalek, J. Hubalek, L. Havel and R. Kizek, *Sensors*, 8 (2008) 445.
59. S. Krizkova, O. Krystofova, L. Trnkova, J. Hubalek, V. Adam, M. Beklova, A. Horna, L. Havel and R. Kizek, *Sensors*, 9 (2009) 6934.
60. O. Krystofova, L. Trnkova, V. Adam, J. Zehnalek, J. Hubalek, P. Babula and R. Kizek, *Sensors*, 10 (2010) 5308.
61. I. Svancara, A. Walcarius, K. Kalcher and K. Vytras, *Cent. Eur. J. Chem.*, 7 (2009) 598.
62. J. Zima, I. Svancara, J. Barek and K. Vytras, *Crit. Rev. Anal. Chem.*, 39 (2009) 204.
63. I. Svancara, K. Vytras, K. Kalcher, A. Walcarius and J. Wang, *Electroanalysis*, 21 (2009) 7.
64. J. Komarek and J. Holy, *Spectroc. Acta Pt. B-Atom. Spectr.*, 54 (1999) 733.
65. M. Konecna and J. Komarek, *Spectroc. Acta Pt. B-Atom. Spectr.*, 62 (2007) 283.
66. M. Konecna, J. Komarek and L. Trnkova, *Spectroc. Acta Pt. B-Atom. Spectr.*, 63 (2008) 700.
67. L. Zalud, Augmented reality user interface for reconnaissance robotic missions, 2007.
68. L. Zalud, L. Kopecny and F. Burian, Robotic systems for special reconnaissance, 2010.
69. L. Zalud, L. Kopecny and F. Burian, Orpheus reconnissance robots, 2008.

70. C. R. Stoker, A. Zent, D. C. Catling, S. Douglas, J. R. Marshal, D. Archer, B. Clark, S. P. Kounaves, M. T. Lemmon, R. Quinn, N. Renno, P. H. Smith and S. M. M. Young, *J. Geophys. Res.-Planets*, 115 (2010) 1.
71. L. K. Tamppari, R. M. Anderson, P. D. Archer, S. Douglas, S. P. Kounaves, C. P. McKay, D. W. Ming, Q. Moore, J. E. Quinn, P. H. Smith, S. Stroble and A. P. Zent, *Antarct. Sci.*, 24 (2012) 211.
72. S. P. Kounaves, R. A. Noll, M. G. Buehler, M. H. Hecht, K. Lankford and S. J. West, in R.B. Hoover, G.V. Levin, R.R. Paepe, A.Y. Rozanov (Editors), Instruments, Methods, and Missions for Astrobiology IV, Spie-Int Soc Optical Engineering, Bellingham, 2001, p. 137.